

Avoiding the polarization catastrophe in LaAlO_3 overlayers on $\text{SrTiO}_3(001)$ through a polar distortion

Rossitza Pentcheva^a and Warren E. Pickett^b

^a*Department of Earth and Environmental Sciences,
University of Munich, Theresienstr. 41, 80333 Munich, Germany and*

^b*Department of Physics, University of California,
Davis, One Shields Avenue, Davis, CA 95616, U.S.A.*

(Dated: October 23, 2018)

A pronounced uniform polar distortion extending over several unit cells enables thin LaAlO_3 overlayers on $\text{SrTiO}_3(001)$ to counteract the charge dipole and thereby neutralize the “polarization catastrophe” that is suggested by simple ion-counting. This unanticipated mechanism, obtained from density functional theory calculations, allows several unit cells of the LaAlO_3 overlayer to remain insulating (hence, fully ionic). The band gap of the system, defined by occupied O $2p$ states at the surface and unoccupied Ti $3d$ states at the interface in some cases ~ 20 Å distant, decreases with increasing thickness of the LaAlO_3 -film before an insulator-to-metal transition and a crossover to an electronic reconstruction occurs at around five monolayers of LaAlO_3 .

PACS numbers: 77.22.Ej, 71.28.+d, 73.20.Hb, 75.70.Cn

Heterostructures containing polar (*e.g.* LaAlO_3 (LAO)) and nonpolar (*e.g.* SrTiO_3 (STO)) oxides raise issues similar to semiconductor heterostructures, *e.g.* Ge/GaAs [1]. If the ionic charges are maintained, then adding LAO layers (with alternating positively charged LaO and negatively charged AlO_2 -layers) onto an STO substrate is expected to lead to an ever-increasing dipole. The accompanying potential shift across the LAO slab should eventually cause a “polarization catastrophe” [2, 3]. To avoid this, surfaces are supposed to reconstruct (atomically, *e.g.* via defects) or facet [4]. However, in oxides containing transition metal ions further compensation mechanisms are available. These can lead to electronic phenomena that are unanticipated from the properties of the bulk constituents and can thus invoke new functionality. Although LAO and STO are two conventional nonmagnetic band insulators, a high conductivity [5] as well as indications for magnetism [6] and superconductivity [7] were measured at the n -type LaO/ TiO_2 interface (IF). The initially reported high carrier density was subsequently found to be sensitive to film growth conditions [2, 6, 8, 9, 10, 11]. Suppressing oxygen vacancies leads to an increase of the sheet resistance by several orders of magnitude [6, 12].

Recently, a thickness dependent switching between insulating and conducting behavior [13] was reported around four monolayers (MLs) of LAO on $\text{STO}(001)$. Thiel *et al.* [13] found that the insulator-to-metal transition can also be induced dynamically by an external electric field. Writing and erasing of nanoscale conducting regions in LAO overlayers on $\text{SrTiO}_3(001)$ was demonstrated [14] with an applied local electric field (by atomic force microscope). In contrast to the abrupt transition in LAO films on

$\text{STO}(001)$, Huijben and collaborators [15] observed a smoother increase in carrier density in coupled p - (hole-doped) and n -type (electron-doped) interfaces where the LAO film was covered by SrTiO_3 . These results lend additional urgency to understand the insulator-to-metal switching in oxide nanostructures.

The seeming violation of charge neutrality has become a central consideration in trying to understand the unexpected behavior that emerges at the interface. So far, theoretical efforts have concentrated mainly on LAO/STO superlattices [16, 17, 18, 19, 20, 21, 22, 23]. For these, density functional theory calculations (DFT) suggest that the charge mismatch at the electron doped n -type interface is accommodated by partial occupation of the Ti $3d$ band. At low temperatures a disproportionation on the Ti sublattice in the interface layer is predicted within LDA(GGA)+U [24] with Ti^{3+} and Ti^{4+} arranged in a checkerboard manner [16, 22, 23].

At first glance the transition from insulating to conducting behavior found between three and four MLs on $\text{SrTiO}_3(001)$ [13] does not fit into the picture obtained from the GGA+U calculations for infinitely extended superlattices [16, 23]. In the latter the charge mismatch is accommodated immediately at the IF and largely independent of the thickness of LAO and STO.

Here we shed light on the nature of the electronic state at the interface and the origin of thickness dependent metal-to-insulator transition. Based on DFT-calculations, we demonstrate that an interface between a thin LAO film on a $\text{STO}(001)$ substrate is fundamentally different from an IF in a periodic superlattice. In a thin overlayer there are two polar discontinuities, one at the IF and another at the sur-

face. As we will show in this paper, the proximity to the surface and the associated atomic relaxation has a profound effect on the properties and compensation mechanism at the interface.

To address these issues, we study here the structural and electronic properties of 1-5 ML of LAO on a STO(001)-substrate, and contrast them with the corresponding behavior at LAO/STO superlattices. The DFT calculations are performed with the all-electron full-potential augmented plane waves (FP-APW) method in the WIEN2k-implementation [25] and generalized gradient approximation (GGA) [26] of the exchange-correlation potential. We have used the lateral lattice constant of the SrTiO₃-substrate obtained from GGA (3.92Å) because it is in closer agreement with the experimental value (3.905Å). Thus the epitaxial LaAlO₃-film (3.79Å) is subject to tensile strain on SrTiO₃ due to a lattice mismatch of 3%. The GGA-gap for bulk SrTiO₃ is 2.0 eV (experimental value 3.2 eV) separating filled O 2*p* bands and unfilled Ti 3*d* bands. For LaAlO₃ we obtain a band gap within GGA of 3.7 eV (experimental value 5.6 eV) between filled O 2*p* bands hybridized with Al *p*-bands and unfilled conduction bands comprised of La 5*d* and Al 3*s*, 3*p* states.

The thin (1-5 ML) LAO films on a STO(001) substrate were modeled in the supercell geometry with two inversion symmetric surfaces to avoid spurious electric fields. To minimize the interaction between neighboring surfaces, the slabs are separated in *z*-direction by 10-12Å of vacuum. Because XRD [27] and LEED [28] measurements give no indication for a superstructure, we have considered only defect-free unreconstructed surfaces. However, we have allowed for more complex symmetry breaking and electronic reconstruction by using a $c(2 \times 2)$ -lateral periodicity. For this cell 15 *k*-points in the irreducible part of the Brillouin zone were used.

Polar distortions. A full structural optimization was performed within the tetragonal unit cell using GGA. The relaxed structures are pictured in Fig. 1 and the atomic displacements which are exclusively along the *c*-axis are plotted in Fig. 2.

An unexpected pattern is uncovered: (i) The surface AlO₂ layer shows an inward relaxation of both Al (0.12-0.19Å) and O (0.11-14Å) atoms by similar amounts, resulting in only a small buckling of 0.01-0.04Å. (ii) The most striking result is a strong buckling in all LaO layers with a uniform polar-type distortion of 0.20-0.36 Å. This relaxation is dominated by the outward movement of La by up to 0.26 Å. (iii) The subsurface AlO₂ layers are also buckled by approx. 0.15 Å: Al relaxes outward by 0.01-0.08 Å, O inward by ~ 0.10 Å. (iv) The Ti and O-ions at the interface show only small outward relaxation (less than 0.06 Å). This situation of large

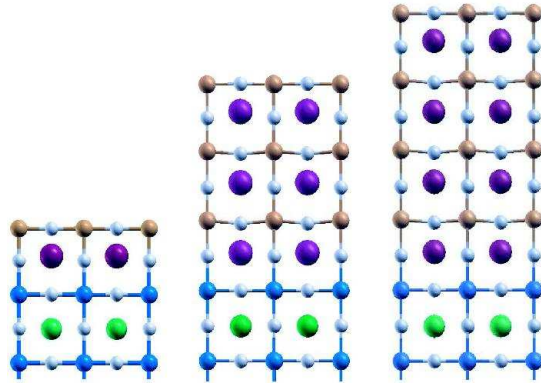


FIG. 1: Side view of the relaxed structures of 1, 3 and 4 ML LAO on STO(001) showing the ferroelectric distortion. The oxygen ions are marked by light grey spheres, while the Sr-, Ti-, La- and Al-cations are shown by green, blue, purple and orange spheres.

polar distortions throughout the LAO slab with negligible distortion in STO contrasts strongly the behavior obtained for LaAlO₃ (or LaTiO₃)/SrTiO₃ superlattices where ferroelectric-like plane-buckling is predominantly in the TiO₂ layer at the interface [17, 18, 19, 20, 29, 30] and amounted to 0.17Å for a 5LAO/5STO heterostructure [23].

Although not explicitly discussed, previous VASP calculations showed a similar relaxation pattern [14]. In contrast, another WIEN2k study reported only small relaxations [31] also finding metallic behavior for all LAO thicknesses. Vonk *et al.*[27] fitted structural models to surface x-ray diffraction (SXRD) data for a LAO overlayer on STO(001) with a total coverage of 0.5 MLs. The best fit infers a contracted TiO₆ octahedron at the interface and an outward relaxation of La in the LaO layer. A direct comparison to our results is not possible because of the different coverage and since the incomplete LAO layer allows for lateral relaxations of strain.

Compensating electronic and ionic dipoles. The implied dipole moment of a 4ML LaAlO₃-film is $D_{bare} \approx -0.5e \times (3.9\text{\AA}) \times 4\text{cells} = -7.8 e\text{\AA}$ which translates into a bare potential shift across the four LAO layer slab of 80-90 eV. This electric field is screened by electronic *plus* ionic polarization. Using the bulk LAO dielectric constant $\epsilon=24$, this becomes approximately $\Delta V = 4\pi e \frac{D_{bare}\epsilon}{\epsilon(3.9\text{\AA})^2} \sim 3.5$ eV, which can be sustained by the 5.6 eV gap of LAO.

The dipole shift due to the polar distortion can be estimated from the displacements, using the formal ionic charges [33]. The layer resolved dipoles, pictured in Fig. 2, show a strikingly uniform behavior in the inner LAO layers (a strong dipole moment of

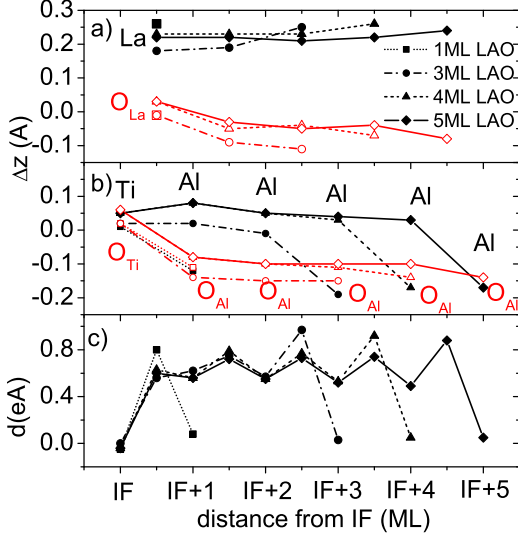


FIG. 2: Vertical displacements of ions Δz with respect to the bulk positions in \AA for 1-5 MLs of LAO on STO(001) obtained within GGA. a) and b) displays the relaxations in the AO and BO₂ layers, respectively with cation/oxygen relaxations marked by full black/open red symbols. The corresponding layer-resolved dipole moments are displayed in (c). The x axis shows the distance from the interface (I) TiO₂-layer.

~ 0.55 and ~ 0.75 e \AA in the AlO₂ and LaO layers, respectively) and an almost vanishing dipole in the interface TiO₂ and surface AlO₂ layers. The total ionic dipole *e.g.* for the 4ML LAO film is:

$$D = \sum Z_i \Delta z_i \approx 4.8 \text{ e}\text{\AA} \quad (1)$$

This rough estimate gives a value that is more than 60% of D_{bare} and of opposite sign. The large polar distortion has a significant impact on the electronic behavior of the system (LAO film + STO substrate).

Electronic properties of overlayer + interface.

The total density of states as a function of the LAO thickness for 1-5 ML thick LAO films on STO(001) is shown in Fig. 3. For the ideal atomic positions all systems are metallic due to an overlap of the surface O 2*p* bands with the Ti 3*d* bands at the interface (cf. Fig. 4). The strong lattice polarization leads to insulating behavior for $N = 1 - 4$ ML. With increasing thickness of the LAO-film the gap decreases by approximately 0.4 eV per added LAO-layer starting from 1.7 eV for 1ML LAO and finally closes for 5 ML LAO/STO(001). While the DFT calculations correctly predict an insulator-to-metal transition, the critical thickness is affected by the band gap underestimation within GGA and is expected to occur beyond an LAO thickness of 6 MLs

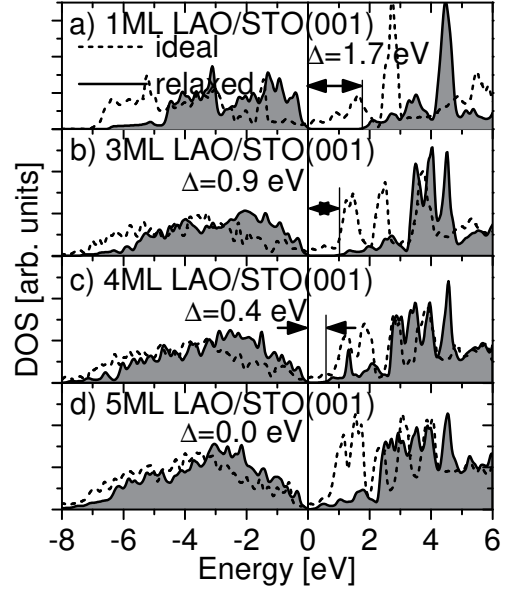


FIG. 3: Density of states for the ideal (dashed line) and relaxed (solid line, grey filling) structure of 1-5 ML LAO on STO(001). Relaxation opens a band gap, but its size decreases with each added LAO layer.

for a defect-free surface. Defects and/or adsorbates which are not considered in the theoretical model may be responsible for the lower critical thickness found in experiment [13].

In order to gain more insight into the type of electronic states around the Fermi level and their spatial distribution, we have plotted in Fig. 4 the layer-resolved density of states for 5ML LAO/STO(001) with ideal and relaxed atomic positions. A nearly rigid upward shift of the O 2*p*-bands towards the Fermi level is observed as they approach the surface. For the relaxed configuration the top of the valence band is determined by the O 2*p* band in the surface AlO₂ layer, while the bottom of the conduction band is fixed by the unoccupied Ti 3*d* band at the interface. Thus, the closing of the gap is due to the raising of the O 2*p* valence band states in the surface LAO layer as the LAO slab gets thicker.

For an isolated IF (in LAO/STO superlattices), the “extra” 0.5*e*⁻ per IF Ti ion must be accommodated, it cannot go into the LAO layers due to the large band gap, and it remains at the IF and charge-orders (within GGA+U) rather than occupy itinerant Ti 3*d* states within the STO layers [16, 23]. In contrast, in thin LAO overlayers, it does not go into the Ti 3*d* states *anywhere*; the lattice screening preserves the formal electronic charges corresponding to closed shells, therefore including correlation effects within LDA+U would not influence the result.

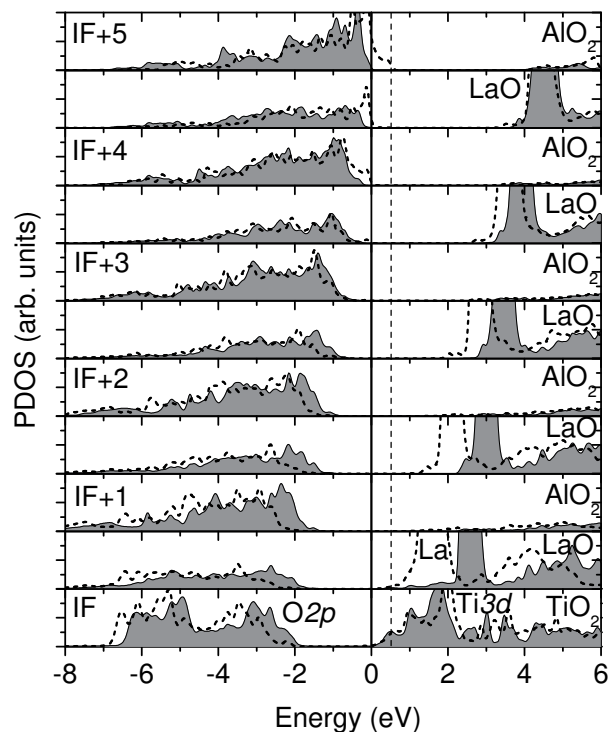


FIG. 4: Layer resolved density of states of 5 ML LAO on STO(001) with ideal (dashed line) and relaxed (grey shaded area) coordinates. The DOS for the ideal positions was shifted by 0.5 eV to align with the conduction band of the system with the relaxed atomic positions. The Fermi level of the unrelaxed system is marked with a dashed line.

Up to a critical LAO thickness of 5ML the ‘extra’ 0.5 electron at the interface appears to have been shifted

to the surface and there is no need for an electronic (or atomic) reconstruction as observed for the superlattice. However, beyond a critical coverage, the system is expected to become metallic.

In summary, strong lattice polarization compensates the dipolar electric field in thin LAO-overlayers and sustains the insulating behavior up to 5 MLs LAO. The effect of this polar distortion is crucial: Without it, the system is metallic for any coverage of LaAlO_3 . The band gap in the relaxed systems formed between the $\text{O}2p$ states in the surface layer and the $\text{Ti}3d$ states at the interface decreases gradually and collapses at 5 ML LAO/STO(001) giving rise to an electronic reconstruction as the system approaches the limit of the isolated interface.

The structural distortion we observe here differs from issues discussed for ultrathin ferroelectric films, *e.g.* the existence of a critical thickness below which ferroelectric displacements are suppressed [34, 35, 36, 37]. In contrast, LaAlO_3 is a wide band gap insulator with a low dielectric constant and no ferroelectric instability. In this case the lattice distortion is driven by the polar nature of the surface. Further examples that nanoscale objects can sustain polarity are recently emerging (see [38] and references therein). In the context of tailoring materials properties for device applications, finite size effects in ultrathin oxide films prove to be an exciting area for future research.

We acknowledge useful discussions with H.Y. Hwang, M. Huijben, J. Mannhart, N. Spaldin and M. Stengel and support through the Bavaria-California Technology Center (BaCaTeC), ICMR, DOE Grant DE-FG03-01ER45876, and a grant for computational time at the Leibniz Rechenzentrum.

-
- [1] W.A. Harrison *et al.*, Phys. Rev. B **18**, 4402 (1978).
 - [2] N. Nakagawa, H. Y. Hwang, and D.A. Muller, Nature Materials **5**, 204 (2006).
 - [3] J. Gonjakowski, F. Finocchi and C. Noguera, Rep. Prog. Phys. **71**, 016501 (2008).
 - [4] P.W. Tasker, J. Phys. C **12**, 4977 (1979).
 - [5] A. Ohtomo and H. Y. Hwang, Nature **427**, 423 (2004).
 - [6] A. Brinkman, *et al.*, Nature Mater. **6**, 493 (2007).
 - [7] N. Reyren, *et al.*, Science **317**, 1196 (2007).
 - [8] W. Siemons, *et al.*, Phys. Rev. Lett. **98**, 196802 (2007)
 - [9] A. Kalabukhov *et al.*, Phys. Rev. B **75**, 121404(R) (2007).
 - [10] P.R. Willmott *et al.*, Phys. Rev. Lett. **99**, 155502 (2007).
 - [11] M. Basletic, *et al.*, Nature Mater. **7**, 621 (2008).
 - [12] G. Rijnders and D. H. A. Blank, Nature Materials **7**, 270 (2008).
 - [13] S. Thiel, G. Hammerl, A. Schmehl, C. W. Schneider, and J. Mannhart, Science **313**, 1942 (2006).
 - [14] C. Cen *et al.*, Nat. Materials **7**, 298 (2008).
 - [15] M. Huijben, *et al.*, Nature Materials **5**, 556 (2006).
 - [16] R. Pentcheva and W.E. Pickett, Phys. Rev. B **74**, 035112 (2006).
 - [17] S. Gemming and G. Seifert, Acta Mater. **44**, 4299 (2006).
 - [18] M.S. Park, S.H. Rhim, and A.J. Freeman, Phys. Rev. B **74**, 205416 (2006).
 - [19] J.-M. Albina, *et al.*, Phys. Rev. B **76**, 165103 (2007).
 - [20] J.-L. Maurice, *et al.*, Mat. Sci. & Eng. B **144**, 1 (2007).
 - [21] K. Janicka, J.P. Velev, and E. Tsybmal, Appl. Phys. Lett. **103**, 07B508 (2008).
 - [22] Z. Zhong and P. Kelly, Eur. Phys. Lett. **84**, 27001, (2008).

- [23] R. Pentcheva and W.E. Pickett, Phys. Rev. B **78**, 205106 (2008).
- [24] V.I. Anisimov, *et al.*, Phys. Rev. B **48**, 16929 (1993).
- [25] P. Blaha, *et al.*, WIEN2k, (K. Schwarz, Techn. Univ. Wien, Austria) 2001. ISBN 3-9501031-1-2
- [26] J. P. Perdew, K. Burke, and M. Ernzerhof, Phys. Rev. Lett. **77**, 3865, (1996).
- [27] V. Vonk, *et al.*, Phys. Rev. B **75**, 235417 (2007).
- [28] W. Moritz, private communication.
- [29] D. R. Hamann, D.A. Muller, H.Y. Hwang, Phys. Rev. B **73**, 195403 (2006).
- [30] S. Okamoto, A. J. Millis, and N. A. Spaldin, Phys. Rev. Lett. **97**, 056802 (2006).
- [31] U. Schwingenschlögl and C. Schuster, Eur. Phys. Lett. **81**, 17007, (2008).
- [32] S. C. Erwin and W. E. Pickett, Solid State Commun. **81**, 891 (1992).
- [33] We note that both the shift by a rigid number of lattice constants and the use of formal charges (or Born effective charges [17] which may be more appropriate) is only a rough estimate.
- [34] D. D. Fong et al., Science **304**, 1650 (2004).
- [35] M. Dawber et al., Phys. Rev. Lett. **95**, 177601 (2005).
- [36] L. Despont et al., Phys. Rev. B **73**, 094110 (2006).
- [37] For a review or overview, see C. H. Ahn, K. M. Rabe, and J.-M. Triscone, Science **303**, 488 (2004); P. Ghosez and J. Junquera, cond-mat/0625299.
- [38] J. Gonjakowski, F. Finocci and C. Noguera, Rep. Prog. Phys.**71**, 016501 (2008).